Differential proteomic expression in non-functional pituitary neuroendocrine tumours and pituitary glands

Nicholas G. Candy[1], Mahnaz Ramezanpour[1], George Bouras[1], Nusha Chegeni[2], Timothy Chataway[2], Rebecca J. Ormsby[3], Alistair K. Jukes[1], Sarah Vreugde[1], Peter-John Wormald[1], Alkis J. Psaltis[1]

Rhinology 62: 6, 750 - 758, 2024
https://doi.org/10.4193/Rhin24.216

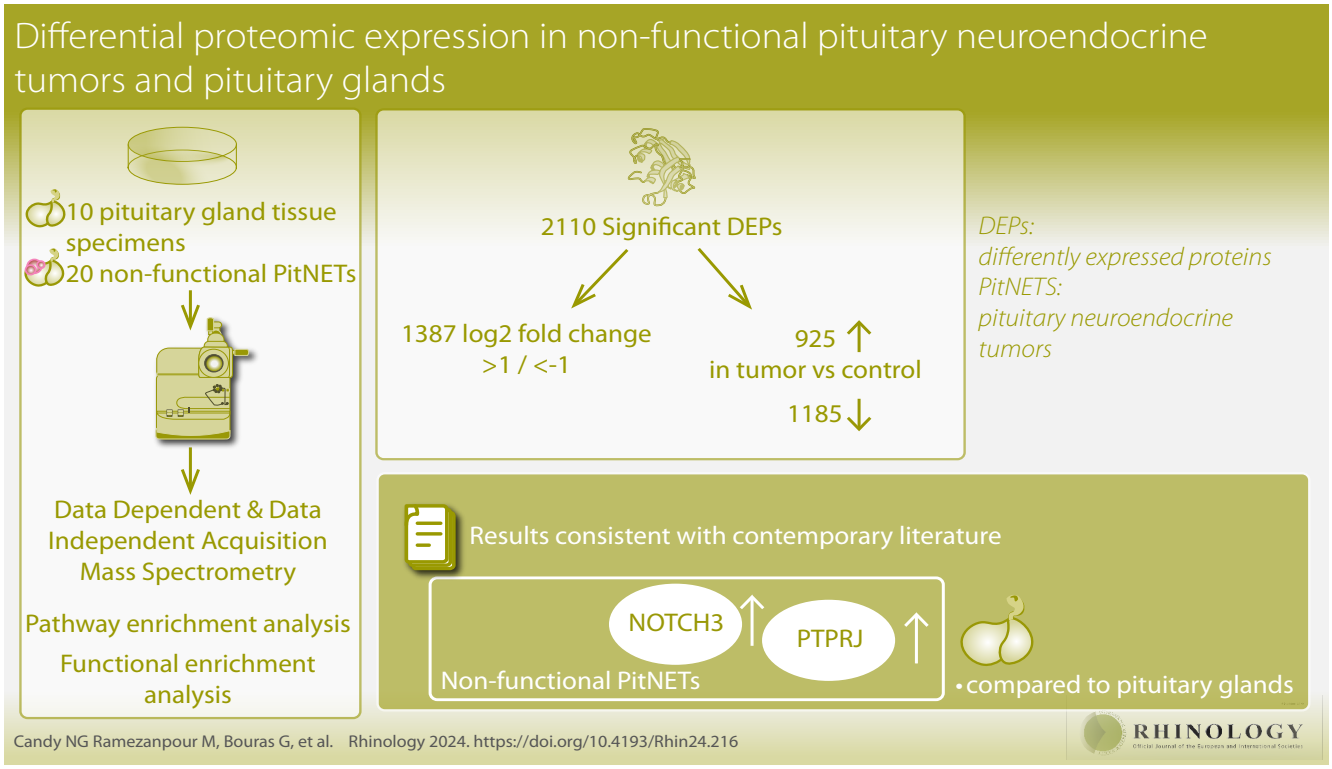

Abstract

Introduction: Pituitary neuroendocrine tumours (PitNETs) are common accounting for 10 to 25 % of all intracranial tumours. This project describes the feasibility of developing a novel membrane-based biomarker that could be used for fluorescent guided surgery. The aim was to catalogue the differential expression of membrane proteins between non-functional PitNETs and pituitary glands. **Methodology**: Ten pituitary gland tissue specimens were obtained from the National Institute of Health (NIH) NeuroBio-Bank and twenty non-functional PitNETs were obtained from the Northwestern University Nervous System Tumour Bank. Mass spectrometry analysis using an Orbitrap Fusion Lumos Tribrid Mass Spectrometer linked to a Dionex Ultimate 3000 UPLC system was undertaken. Data Dependent Acquisition Mass Spectrometry and Data Independent Acquisition Mass Spectrometry was then completed. Pathway enrichment analysis was performed using clusterProfiler v4.6.0. Functional enrichment analysis was conducted using Gene Ontology terms and Reactome pathways. **Results**: Differential expression analysis between the two groups revealed a total of 2110 significant differently expressed proteins (DEPs), with 1387 of these also having a Log2 fold change either greater than 1, or less than -1. Of the 2110 DEPs, 925 were upregulated in tumours compared to control, while 1185 were down-regulated. **Conclusion**: We have demonstrated a proteomic comparison between non-functional PitNETs and normal pituitary glands. These results demonstrate differences consistent with contemporary literature but shows that NOTCH3 and PTPRJ are up-regulated in non-functional PitNETs compared to pituitary glands

Key words: pituitary neuroendocrine tumour, membrane receptors, surgical fluorescence imaging

Introduction

Pituitary neuroendocrine tumours (PitNETs) are common, accounting for 10 to 25 % of all intracranial tumours [1]. PitNETs are classified clinically as functional or non-functional [1]. Functional PitNETs cause symptoms due to hypersecretion of pituitary hormones that manifest particular clinical syndromes, whereas non-functional PitNETs cause symptoms due to continued growth resulting in compression of surrounding structures, such as the optic nerves [2].

PitNETs are considered to originate from monoclonal/oligoclonal somatic genetic mutations or chromosomal abnormalities, with 95 % of cases being sporadic and 5 % of cases being familial [3]. In sporadic cases the somatic alterations in oncogenes, tumour suppressor genes and transcription factors have only been identified in about 60 % of cases.

Contemporary surgical management through an endoscopic transsphenoidal resection achieves a gross total resection rate between 70% to 80% [4,5]. Similar rates of pituitary preservation or hormone remission are achieved for non-functional and functional PitNETs, respectively [6]. Increasing surgical experience does improve these outcomes however, the learning curve is long [7]. Additional intraoperative techniques that augment the degree of resection and endocrine outcome for patients undergoing endoscopic surgery for non-functional PitNETs is needed.

The development of molecular tracers for fluorescence guided oncological surgery is an area of active research [8]. Phase III trials have demonstrated improved resection margins in patients who underwent fluorescence guided resection. Importantly, the increased rates of resection translated into improved progression free survival [9-11]. Clear delineation of the plane between tumour and normal pituitary gland is important for patients undergoing pituitary surgery. The ability to recognise this plane intraoperatively can improve endocrine outcomes by facilitating pituitary gland preservation [12].

Specific accumulation of a fluorescent agent requires the identification and development of a molecule which binds to the target tissue. This molecule is then conjugated with a fluorophore, like indocyanine green, which can be detected with near-infrared cameras. Current research into fluorescence guided pituitary surgery has focused on fluorescent agents that have been used in other solid tumours, such as OTL 38 [13]. This has shown sensitive detection in non-functioning PitNETs that demonstrate folate receptor alpha (FRα)expression. However, not all tumours demonstrate FRα expression which may limit its generalisability. Determining novel membrane-based biomarkers that could be used for tumour specific imaging is clearly needed. The first step in this process would be developing a catalogue of the membrane proteins and their differential expression between non-functional PitNETs and pituitary glands, as this would allow development of a molecular that targets these tumours with high sensitivity and specificity.

Materials and methods

Ten control pituitary gland tissue specimens were obtained from the National Institute of Health (NIH) NeuroBioBank and twenty non-functional PitNETs were obtained from the Northwestern University Nervous System Tumour Bank. Patients provided informed consent for tissue or tumour donation. This study had local institutional ethics approval (CALHN Reference Number 16411).

The control pituitary gland tissue samples were donated from patients of varying ethnicity (six white, two Asian, one black, one unknown) with ages ranging from 21 to 82. The average post-mortem time interval was 15 hours, with a range from 4 hours to 47 hours. Patients were specifically selected from the respective tissue banks ensuring they had no documented co-morbidities that could affect their pituitary gland function, such as being on anti-psychotic medication or having a co-existing PitNET.

The non-functional PitNET samples were donated from fresh frozen intraoperative samples. All patients had clinically non-functional tumours and did not manifest an endocrine hypersecretion syndrome. The immunohistochemistry for the associated pituitary gland hormones was completed as part of routine histopathological analysis at Northwestern University. The results of the histopathological report were provided in addition to the tissue specimens. The results are demonstrated in Table 1. Transcription factors were not routinely tested for all samples during the time these tumour specimens were collected between 2014 to 2021. Therefore, the histopathological classification according to the WHO 2021 guidelines is not possible.

Digestion and proteomics analysis

100 mg of tissue were lysed in 500 µl of RIPA buffer with a 1X cocktail of protease inhibitors (Thermo Fisher Scientific, Waltham, USA) using a Qiagen TissueLyser II (Qiagen, Hannover, Germany) for 10 minutes. The samples were then centrifuged at 45,000 RPM for 30 minutes at 4°C. The supernatant (protein extract) was transferred into a fresh maximum recovery tube (Axygen, China). The protein concentration was assessed using the NanoOrange Protein Quantitation Kit (Thermo Fisher Scientific, N6666) according to the manufacturer's instructions.

In the preparation of proteins for analysis, they underwent an initial reduction with tris (2-carboxyethyl) phosphine (TCEP) at a concentration of 10 mM and were subjected to a temperature of 56°C for 30 minutes. Following this, the proteins were alkylated using chloroacetamide (Sigma-Aldrich, St Louis, USA) at a concentration of 20 mM, conducted in darkness at room temperature for 30 minutes. Glass spheres (Sigma-Aldrich, USA Catalogue number 440345) were washed and adjusted to a final concentration of 50 mg/ml in Acetonitrile in water [14]. The Bead mixture was added to the reduced and alkylated protein samples at a 10 to 1 bead to protein molar ratio resulting in protein precipitation onto the beads. Samples were then washed thrice with 80

Table 1. Immunohistochemistry results for staining of major pituitary hormones for the 20 non-functional PitNETs that were examined.

Specimen number	FSH	ACTH	LH	TSH	Prolactin	GH
1	focal positivity	focal positivity	negative	negative	negative	not reported
2	negative	patchy positivity	negative	negative	negative	patchy positivity
3	negative	negative	negative	negative	rare positive tumour cells	positive
4	negative	negative	negative	negative	negative	negative
5	patchy positivity	negative	rare positivity	patchy positivity	negative	negative
6	negative	few scattered positive cells	negative	negative	negative	negative
7	positive	negative	positive	negative	negative	negative
8	positive	negative	positive	negative	negative	negative
9	negative	negative	negative	negative	negative	negative
10	moderate to strong positive	negative	scattered positive cells	negative	not reported	negative
11	rare positivity	negative	weakly positive	negative	negative	negative
12	positive	negative	positive	negative	negative	negative
13	positive	negative	positive	negative	negative	negative
14	negative	rare positive cells	negative	negative	negative	negative
15	negative	negative	negative	negative	negative	negative
16	negative	negative	negative	positive	negative	negative
17	negative	negative	positive	negative	negative	positive
18	weak, patchy positivity	negative	diffuse, patchy positivity	negative	negative	negative
19	negative	negative	negative	negative	rare positive	rare positive
20	negative	negative	negative	negative	negative	negative

FSH; follicle stimulating hormone, ACTH; adrenocorticotroph hormone, LH; luteinizing hormone, TSH; thyroid stimulating hormone, GH; growth hormone.

% ethanol as per the manufacturer's instructions. Subsequent digestion of the precipitated proteins utilized trypsin at an enzyme-to-substrate ratio of 1:20 (Promega, Madison, USA) and incubation overnight at 37°C. The resulting peptides underwent precipitation using C18 StageTip Cleanup (Thermo Fisher Scientific), following the manufacturer's protocol. Following drying, the sample was resuspended in MS water with 5% acetonitrile to achieve a final peptide concentration of 1 µg/3 µl, in readiness for mass spectrometry acquisition. To ensure the representation of all peptides in the chromatogram library, aliquots from all samples were combined.

LC-Mass Spectrometry

For mass spectrometry analysis, an Orbitrap Fusion Lumos Tribrid Mass Spectrometer (Thermo Fisher Scientific, USA) was linked to a Dionex Ultimate 3000 UPLC system (Thermo Fisher Scientific). Peptides were initially loaded onto a custom-made trap measuring 150µm x 5 mm with 1.5 µm C18 (Flinders Omics Facility) and subsequently separated using a custom-made 75 µm (inner diameter) analytical column featuring an integrated pulled-tip emitter. The column was packed with ReproSil-Pur 120 C18-AQ beads (1.9 µm, 120 Å, Dr. Maisch, Ammerbuch, Germany) and extended to 40 cm (Flinders Omics Facility). Each injection comprised 1 µg of peptides, loaded and separated over a 210-minute gradient ranging from 3% to 31.2% buffer B (0.1% formic acid in 80 % acetonitrile). This was succeeded by a 30-minute wash gradient and equilibration step.

Data Dependent Acquisition Mass Spectrometry (DDA-MS) and Data Independent Acquisition Mass Spectrometry (DIA-MS)

DDA-MS Gas-phase fractionation (GPF) was employed to construct a spectral library for DIA analysis. Pooled samples, consisting of 1.5 µL from each sample digest, underwent six GPF library acquisitions. Each acquisition covered a specific narrow m/z range within the 350 – 1200 m/z mass range (350-500m/z for method 1, 490-610m/z for method 2, 600-710m/z for method 3, 700-810m/z for method 4, 800-910m/z for method 5,

900-1200m/z for method 6). For each DDA-GPF analysis, 1 µg of the pooled sample was used, employing a 3-second cycle time instrument method, MS1 resolution of 60,000, auto maximum injection time mode, and a normalized AGC target of 200%. The MS2 resolution was set to 30,000 with an intensity threshold of 5.0e5, dynamic exclusion duration of 60 seconds, 400% normalized AGC target, and 30% normalized HCD collision energy with dynamic maximum injection time mode.

In preparation for DIA analysis, the Orbitrap Fusion Lumos Tribrid Mass Spectrometer was set up with an MS1 scan range spanning 350-1200 m/z, a resolution of 120,000, a normalized AGC target set at 200%, and dynamic maximum injection time mode. For MS2, a series of variable-sized isolation windows was utilized for fragmentation, maintaining an orbitrap resolution of 30,000. The normalized AGC target was set at 2000%, with dynamic maximum injection time mode, and a consistent normalized HCD collision energy of 30% for all DIA scans.

Protein identification, quantification, and DIA data analysis

The DIA spectra were processed and quantified using Spectronaut v15 (Biognosis AG, Schlieren, Switzerland) with factory default settings. Differential protein expression analysis was performed in R v4.2.0 [15] using the DEP package v1.20.0 to calculate differentially expressed proteins (DEP) [16]. Specifically, data was normalised with the variance stabilising transformation vsn using the DEP package's 'normalize_vsn' function. Proteomic expression differences between the tumour and control samples were tested using the DEP package's 'test_diff' function that implements Limma v 3.54.2 [16]. Control was used to refer to pituitary gland samples and PitNETs were referred to as tumour samples.

Functions from the tidyverse collection of R packages v 1.3.2 were incorporated into the analysis and visualisation. The threshold for identifying differentially expressed proteins was set at a false discovery rate (FDR) of less than 0.1.

Pathway enrichment analysis is a bioinformatic method of determining specific biological pathways that are persistently perturbed in omics data, such as from this proteomics experiment [21]. The are three major phases involved in pathway enrichment analysis [21,22]. The first step involves defining and linking biological pathways to their constituent gene/protein lists using curated databases. In this case we selected the Gene Ontology (GO) database and Reactome pathway database. The second step involves pathway enrichment analysis which utilises statistical methods to identify pathways that are upregulated or downregulated compared to a control group. This is done by assessing whether the genes within each pathway are over-expressed or under-expressed, relative to what is expected by chance. For example, if many proteins belonging to a certain biological pathway are consistently have higher expression in the treatment group compared to the control group, this pathway would be upregulated in the treatment group. The third step involves visualisation and interpretation of the pathway enrichment results, which we discuss at the end of this section and include in Figures 1 and 2.

Pathway enrichment analysis was performed using clusterProfiler v4.6.0 (Wu et al., 2021) [18]. Functional enrichment analysis was conducted using Gene Ontology (GO) terms and Reactome pathways [19,20].

Over representation analysis (ORA) of GO terms was conducted by taking all significant differentially expressed proteins (padj <0.1) and splitting them into down- (Log2 fold change < 0) and up-regulated (Log2 fold change > 0) groups. The 'gseGo' function from clusterProfile was used for all tests against a background of all 6492 detected proteins, with a minimum pathway set size of 10 and maximum pathway set size of 500.

Gene set enrichment analysis (GSEA) was conducted on the list of genes, sorted by their Log2 fold changes using the clusterProfiler 'enrichGo' and 'enrichPathway' functions against a background of all 6492 detected proteins, with a minimum pathway set size of 10 and maximum pathway set size of 500. The GOSemSim R package was used to reduce redundancy among enriched GO terms, with a threshold of 0.7 [20] using the 'simplify' function.

The Benjamini-Hochberg method was used for p-value adjustment for all functional enrichment analyses, accounting for multiple testing, with a false discovery rate (FDR) of 0.1 as denoting significance. A t test was used to compare the mean number of detected proteins between control and tumour samples, with a significance of α=0.05 selected.

Results

Overview

Data-independent acquisition mass spectrometry (DIA-MS) was performed. A total of 28 out of 30 samples passed quality control (QC). A total of 6492 unique proteins were detected across all samples. The minimum number of proteins detected in any sample was 4325, while the maximum was 6154. Not all proteins were detected in all samples, explaining why the total number of proteins detected is greater than the maximum number of proteins detected in a single sample. There were significantly fewer proteins on average in PitNET samples comparted to pituitary glands (t-test = 0.002. PitNET mean = 5343, pituitary gland mean = 5804). A total of 3281 proteins were present in all 28 samples.

Principal components analysis of the top 250 most variable proteins clearly separated the proteomes of the PitNET samples from the pituitary glands in the first 2 components explaining the most variance (1st component explained 25.1% of the variance, 2nd component 22.3% of the variance) (Figure 1A). Differential expression analysis of all 6492 proteins between the two groups revealed a total of 2110 significant differently expressed

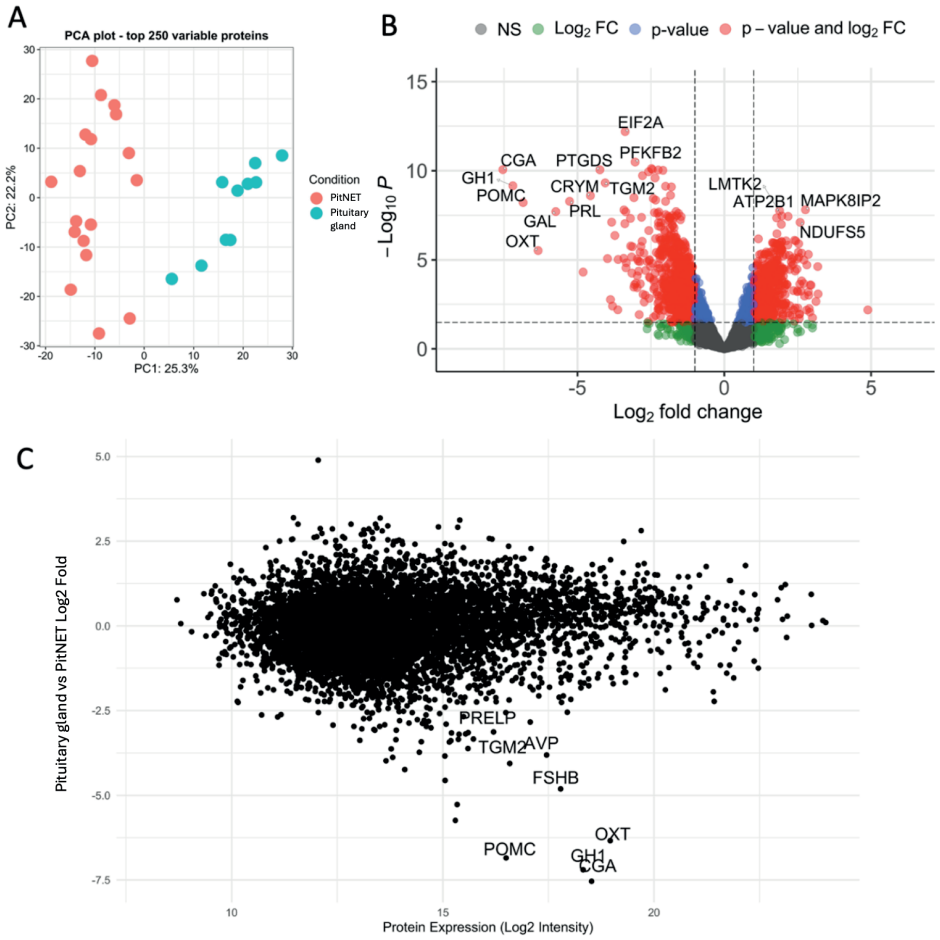

Figure 1. Proteomic analysis of expressed proteins by 18 non-functional PitNETs and 10 pituitary gland samples. (A) Principal component analysis plot based on the top 250 most variable proteins. All PitNETs are coloured in red, pituitary gland tissue samples in blue. (B) Volcano plots showing the log2 fold change (x-axis) and log10 unadjusted p-values (y-axis) of 6492 detected proteins between PitNETs and pituitary gland. Each point is a protein. Proteins on the right side of the plot are upregulated in PitNET tissue compared to pituitary gland, proteins on the left are downregulated. Proteins in red have significantly different protein expression (padj < 0.1) and have an absolute Log2 fold change greater than 1. Proteins in blue have significantly different protein expression (padj < 0.1) with an absolute Log2 fold change less than 1. Proteins in green have an absolute Log2 fold change greater than 1 but are not significantly differentially expressed (padj > 0.1). Grey proteins are neither significantly differentially expressed (padj > 0.1) an absolute Log2 fold change greater than 1. (C) Plot showing protein expression (Log2 intensity) on the x-axis compared to the Log2 fold change between PitNET and pituitary gland. Each point is a protein.

proteins (DEPs) (padj < 0.1), with 1387 of these also having a Log2 fold change either greater than 1, or less than -1 (Figure 1B). Of the 2110 DEPs, 925 were upregulated in PitNET samples compared to pituitary glands, while 1185 were downregulated (Figure 1B).

Pathway analysis

To investigate whether DEPs observed were associated with biological pathways or were randomly distributed, we conducted pathway analysis using over representation analysis (ORA) and gene set enrichment analysis (GSEA) using GO Ontology terms and Reactome terms. A total of 158 significant GO terms (post simplification) were revealed in the 1185 down-regulated gene set, while 76 were significant in the 925 up-regulated gene set. Of the 158 down regulated GO terms they were distributed between 94 biological processes, 41 cellular components and 23 molecular functions whereas, for the 76 up-regulated sets there were a total of 42 biological processes, 22 cellular components and 12 molecular functions.

Examining cellular components GO:0098590 was represented by 10.6% of all down regulated genes. This group of genes is involved with synaptic vesicle docking during exocytosis such as Syntaxin Binding Protein 3 (STXBP3), Phospholipid Phosphotase 3 (PLPP3), Annexin A1 (ANXA1) and Tight Junction Protein 1 (TJP1). Finally, GO:0030117 and GO:0048475 both represent proteinaceous coats that associate with plasma cell membrane.

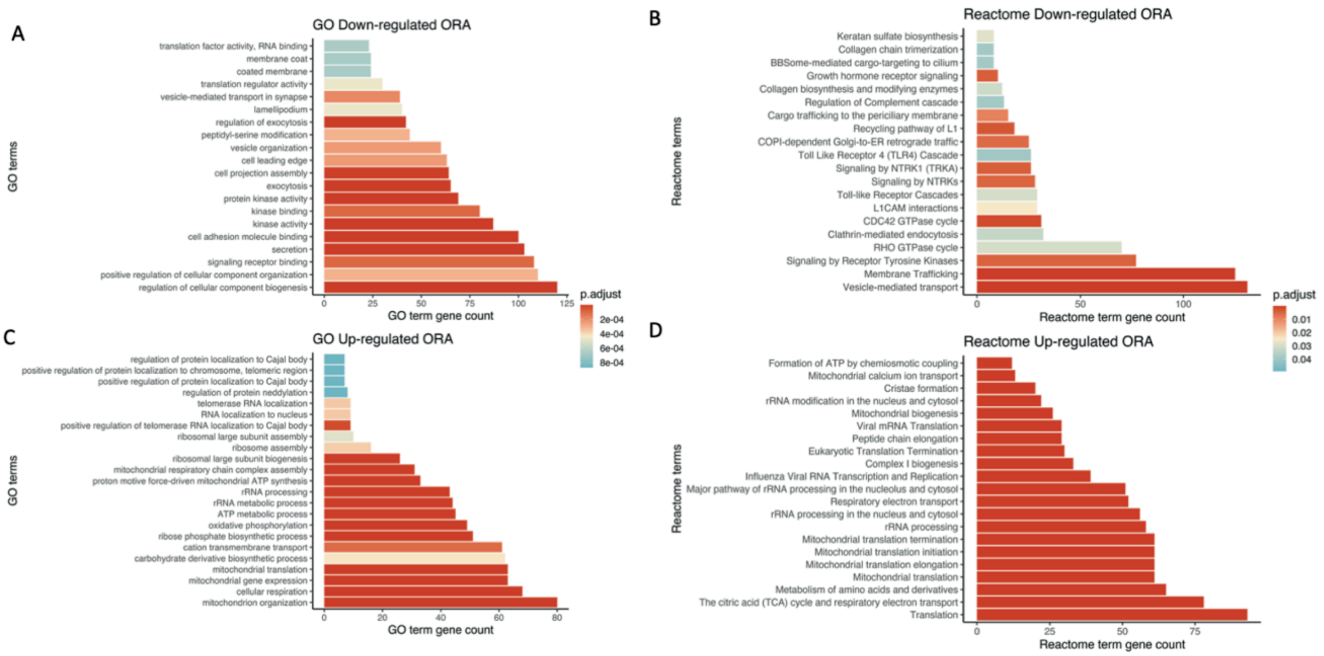

Figure 2. Top 20 Overrepresentation Analysis (ORA) pathways for down-regulated DEPs for GO terms (A) and Reactome terms (B) and up-regulated DEPs for GO terms (C) and Reactome terms (D).

In samples where these proteins were detected they represented 24 of 881 down regulated genes. Alternatively, upregulated cellular component gene sets related to mitochondria and cellular respiration.

A significantly down regulated gene set was identified for molecular functions involving cell adhesion molecule binding (11.4% of all down regulated genes) and signalling receptor binding (12.2% of down regulated genes). These included Prolactin (PRL), Proopiomelanocortin (POMC), Oxytocin (OXT), Vasopressin (AVP) and Gylcoprotein Hormones Alpha Chain (CGA). Alternatively, an upregulated gene set was involved in structural constituent for ribosomes (10.9% of all up regulated genes). Examining biological processes shows a significant number of down regulated gene sets involved in regulation of cellular component biogenesis, secretion, positive regulation of cellular component organisation, negative regulation of protein metabolic processes, negative regulation of molecular function and regulation of cell differentiation. Involved genes included: B-Raf proto-oncogene, serine/threonine kinase (BRAF), Phosphoinositide-3-kinase regulatory subunit 1 (PIK3R1), Mechanistic Target of Rapamycin (MTOR), POMC, OXT, AVP and Mitogen-Activated Protein Kinase (MAPK). The most significant gene sets that were upregulated involved mitochondrial translation and mitochondrial organisation.

Examining specific genes based on the mean expression log fold change that some of the genes with the highest increased regulation in pituitary adenomas compared to pituitary glands included: Keratin 82 (KRT82), Mitochondrial Genome-Encoded ATP Synthase Membrane Peripheral Stalk Subunit (MGARP), Nectin Cell Adhesion Molecule 3 (NECTIN3), Mitochondrially Encoded ATP Synthase Membrane Subunit 8 (MT-ATP8). From those, only NECTIN3 is present on the cell membrane. Whereas, the most down regulated genes in pituitary adenomas compared to pituitary glands included: CGA, Growth Hormone 1 (GH1), POMC, OXT, Galanin and GMAP prepropeptide (GAL), PRL, Follicle Stimulating Hormone Beta Subunit (FSHB), Transglutaminase 2 (TGM2), Erb-B2 Receptor Tyrosine Kinase 2 (ERBB2), Collagen Type I Alpha 2 Chain (COL1A2), AVP, Breast carcinoma amplified sequence 3 (BCAS3), Dickkopf WNT signaling pathway inhibitor 3 (DKK3), Glial Fibrillary Acidic Protein (GFAP), and Annexin A1 (ANXA1). Of those only TGM2 and ANXA1 are expressed on the cell membrane.

For the Reactome terms, the top 20 is shown in Figure 2A and 2C. These include terms relating to 'signalling receptor binding', 'secretion' and 'kinase activity' in the down-regulated set (Figure 2A), and 'cellular respiration', 'mitochondrial translational' and 'localisation to Cajan body' in the up-regulated set (Figure 2C). For the Reactome pathways, there were a total of 54 significant terms from the down-regulated protein set and 31 from the up-regulated set. These included 'membrane trafficking' and 'vesicle-mediated transport' in the down-regulated set (Figure 2B) and 'translation', 'metabolism of amino acids' Looking specifically at genes that were anticipated to be differentially expressed such as the growth hormone receptor and transforming growth factor beta receptor. Growth Factor Receptor-Bound Protein 2 (GRB2) was detected in all pituitary glands and PitNETs but was

down regulated in pituitary adenomas compared to control with a fold change of -0.5 and a mean expression of 13.897. This was not significantly different between the groups. Transforming Growth Factor Beta Receptor 3 (TGFBR3) was detected in all pituitary glands and only nine of the PitNETs. The gene was down regulated with a fold change of -0.21 in pituitary adenomas and a mean expression of 13.7, which was also not significantly different.

Protein Tyrosine Phosphatase, Receptor Type J (PTPRJ), TNF Receptor-Associated Protein 1 (TRAP1) and Notch Receptor 3 (NOTCH3) were membrane bound proteins that were significantly differentially expressed. PTPRJ was detected in all pituitary glands and all the PitNETs. It was upregulated in the PitNETs with a log fold change of 1.22 and a mean expression of 14.77. TRAP1 was detected in all pituitary glands and all the PitNET specimens. It was upregulated in the PitNETs with a log fold change of 0.682 and a mean expression of 15.977. NOTCH3 was detected in all pituitary glands and eleven of the PitNET specimens and were upregulated with a log fold change of 2.8 and a mean expression of 13.564.

Discussion

The molecular pathogenesis of PitNETs is complex and currently not well understood. This is why large multi-omics studies examining different PitNET subtypes are important. The purpose of this project was to identify cell membrane bound molecular markers that could be potentially used in tumour specific imaging. These results demonstrate a first principles approach by identifying the differentially expressed proteins between pituitary gland and non-functional pituitary adenomas and considering these membrane proteins as targets for tumour specific imaging.

Our results demonstrated a total of 2110 significant differently expressed proteins (DEPs) between PitNET samples and normal pituitary glands, with 1387 of these also having a Log2 fold change either greater than 1, or less than -1. Further analysing these DEPs using pathway analysis revealed a total of 158 significant GO terms (post simplification) in the down-regulated gene set, while 76 were up-regulated in PitNETs compared to pituitary glands. These results were supported by contemporary work completed by Banerjee et al. [23]. and Zhang et al. [24].

A landmark study by Zhang et al. [24] in 2022 demonstrated a new integrated proteogenomic classification using the major histological subtypes of PitNETs. They examined the entire genome, transcriptome, proteome and phosphoproteome of 200 PitNETs. They then validated the identified biomarkers on an independent cohort of 750 patients with PitNETs. They identified several potential molecular therapeutic targets: GNAS, CDK6, TWIST1, ZEB2, PDL1, EGFR, EGFR T693 and VEGFR.

Examining the same molecular targets identified in Zhang et al. [24]. Our study detected GNAS in ten PitNETs and ten pituitary glands with a fold change of 0.216 from PitNETs to pituitary glands and mean expression of 14.435, with no significant difference between the two groups (padj=0.846). In addition, CDK6 was detected in eight pituitary glands and seventeen PitNETs with a fold change of 0.625 from PitNETs to pituitary glands and a mean expression of 12.2. EGFR was detected only in three pituitary glands and no PitNETs with a mean expression of 10.717. TWIST1, ZEB2, PDL1 and T693 were not detected.

The similarity between these results is promising. The variation is likely due to the significant number of functional PitNETs tested by Zhang et al. [24] as well as the primary goal of their paper being to identify an integrated molecular classification for PitNETs through a multi-omics approach. Therefore, they may have identified biomarkers that were not identifiable with the proteomic approach used in this analysis as the purpose of their paper was to identify novel diagnostic and therapeutic options for all types of PitNETs.

Banerjee et al. [23] in 2023 published the first matched pituitary proteome for anterior and posterior pituitary glands. They demonstrated that growth hormone and thyroid stimulating hormone are exclusive to the anterior pituitary gland whereas, oxytocin-neurophysin 1 and arginine vasopressin are exclusive to the posterior lobe. Additional proteins were identified such as POU Class 1 Homebox 1 (POU1F1), POMC, Procollagen C-Endopeptidase Enhancer 2 (PCOLCE2) and Neuronal Pentraxin 2 (NPTX2). Interestingly S100 tumour marker protein was found in high expression in the posterior lobe. In our results, POU1F1, PCOLCE2 and NPTX2 were detected in all the pituitary gland specimens, but were only detected in six, fourteen and seventeen of the PitNETs respectively. All three genes were not significantly different between tumour and glands.

Examining significantly differentially expressed proteins included GH1, which was detected in all pituitary glands and PitNETs with a fold change of -7.2 comparing PitNETs to pituitary glands. Thyroid stimulating hormone had a mean expression of 18.3, which was significant. In addition, OXT, AVP and POMC were significantly differentially expressed between PitNETs and pituitary glands. This is anticipated as non-functional PitNETs will most likely have lower expression of these pituitary gland hormones.

Previous research by Evans et al. [25,26] using DNA microarray analysis, Western blotting and immunochemistry demonstrated that Folate Receptor alpha (FRα) is overexpressed in non-functioning PitNETs. Cho et al. [13] investigated a folate receptor antibody conjugated to an indocyanine green fluorophore (originally developed for tumour specific imaging in ovarian surgery) demonstrated 100% sensitivity and specificity for patients that had non-functional PitNETs expressing FRα. Unfortunately, only 9 of the 14 patients with PitNETs had tumours that overexpressed FRα, limiting the usefulness. Nonetheless they did demonstrate that the technique of near infrared (NIR) hardware can be integrated into the surgeon's workflow for endoscopic

endonasal transsphenoidal surgery for resection of pituitary adenomas. FOLR1, the gene that codes for folate receptor was not detected in our results.

A single centre, non-randomised, non-blinded feasibility and dose exploration study is currently being undertaken to investigate bevacizumab-800CW [27]. No results are published yet, but our results did not detect a significant difference between VEGFR expressed on non-functioning PitNETs and pituitary glands. Other non-targeted surgical fluorescence has been investigated using different injection techniques with indocyanine green, however it appears to lack the sensitivity of molecular targeted surgical fluorescence [28].

Compared to non-functional PitNETs, previous studies have identified genomic aberrations that may be found in functional PitNETs. For instance, mutations in ubiquitin specific peptidase 8 (USP8) gene account for 20-60 % of adrenocorticotrophic hormone (ACTH) secreting PitNETs (Cushing's disease). These represent a low proportion of all PitNETs encountered clinically but are challenging cases to manage because gross total resection is required to achieve hormone control [29]. These tumours often present as microadenomas (<10mm) making intraoperative identification and gross total resection challenging. Given the molecular pathogenesis of each subtype of functional PitNET is different, this study is not applicable given we only utilised non-functional PitNETs.

Our results demonstrated that membrane receptors NOTCH3, TGFBR3 and PTPRJ are differentially expressed between non-functional PitNETs and pituitary glands. Anticipated membrane receptors that were not detected in this experiment included Dopamine Receptor 2 (DRD2), Corticotrophin Releasing Hormone Receptor 1 (CRHR1) and Gonadotropin Releasing Hormone Receptor (GNRHR) as these are the receptors that are involved with regulation of the secreted pituitary hormones. Given the significant down regulation of genes that encode for the synthesis of the specific pituitary hormones in PitNETs compared to pituitary glands, it would be expected that the genes encoding for the associated receptors would also be down regulated. This discrepancy may relate to the specific topology of each of these membrane receptors and the method of protein extraction used for mass spectrometry analysis.

NOTCH 3 and PTPRJ were both upregulated in non-functional PitNETs compared to pituitary glands. Future research confirming the membrane localisation of these proteins and the rate of differential expression would be valuable.

Limitations

An obvious limitation of this study was sample size with only a small cohort of PitNETs and glands analysed. Furthermore, it should be recognized that the tissues being compared were collected differently. Tumour samples were collected fresh during surgery and then immediately frozen for use later. Whereas pituitary glands were harvested post-mortem from donors at a variety of times. This may have affected the results in a way that could not be accounted for Blair et al. [30], who in 2016 demonstrated that most proteins in brain tissue remains unchanged even after a post-mortem interval of over 50 hours. Therefore, the potential influence of this limitation would be anticipated to be minor.

A potential confounder relates to the pituitary gland tissue used in the analysis. As stated, the NIH Neurobiobank provided 250mg of pituitary gland tissue from specimens in the biobank. The component of this tissue which represented anterior vs posterior gland is not known. Therefore, some of the pituitary glands analysed may have included posterior pituitary gland. Ultimately, this is of limited consequence given the purpose of the study was to explore potential biomarkers differentially expressed between non-functional PitNETs and pituitary gland.

Conclusion

We have demonstrated a proteomic comparison between non-functional PitNETs and normal pituitary glands. These results demonstrate differences consistent with contemporary literature but shows that NOTCH3 and PTPRJ are up-regulated in non-functional PitNETs compared to pituitary glands. Further research into these receptors for tumour specific imaging may yield promising results.

Acknowledgement

Human pituitary gland tissue obtained from NIH Neurobiobank. Human non-functional pituitary adenoma tissue obtained from Nortwestern University Nervous System Tumour Bank. Specimens for optimisation of the proteomic analysis were obtained from the South Australian Neurological Tumour Bank.

Authors' contributions

Conception. NGC, PJW, AJP
Design. NGC, MR, NC, TC, SV, AJP
Experimental data collection. NGC, MR, GB, NC, TC, RJO
Analysis. NGC, GB, AKJ, PJW, AJP

Funding

This project received funding from the Neurosurgical Research Foundation as part of a Research Scholarship.

Conflicts of interest

No conflicts to declare.

Data availability

Raw data is available as .csv (Excel) files from the website of Rhinology

References

1. Gittleman H, Ostrom QT, Farah PD, Ondracek A, Chen Y, Wolinsky Y, et al. Descriptive epidemiology of pituitary tumors in the United States, 2004-2009. J Neurosurg. 2014;121(3):527-535.
2. Whyte E, Nezu M, Chik C, Tateno T. Update on current evidence for the diagnosis and management of nonfunctioning pituitary neuroendocrine tumors. Endocrinol Metab. 2023;38(6):631-654.
3. Vamvoukaki R, Chrysoulaki M, Betsi G, Xekouki P. Pituitary tumorigenesis-implications for management. Medicina. 2023;59(4).
4. Candy NGJA, Ooi EH, Valentine R, et al. The evolution of pituitary surgery in an Australian health care framework. J Neurol Surg B Skull Base. 2024. (efirst)
5. Hussein Z, Grieve J, Dorward N, et al. Non-functioning pituitary macroadenoma following surgery: long-term outcomes and development of an optimal follow-up strategy. Front Surg. 2023;10:1129387.
6. Candy NG, Ovenden C, Jukes AK, Wormald PJ, Psaltis AJ. The learning curve for endoscopic endonasal pituitary surgery: a systematic review. Neurosurg Rev. 2023;46(1):241.
7. Candy NG, Jukes AK, Van Der Veken J, Torpy DJ, Vrodos N, Santoreneos S, et al. The learning curve for endoscopic endonasal transsphenoidal pituitary surgery: evaluating endocrine outcomes. J Clin Neurosci. 2024;120:14-22.
8. Hernot S, van Manen L, Debie P, Mieog JSD, Vahrmeijer AL. Latest developments in molecular tracers for fluorescence image-guided cancer surgery. Lancet Oncol. 2019;20(7):e354-e67.
9. Grossman HB, Stenzl A, Fradet Y, et al. Long-term decrease in bladder cancer recurrence with hexaminolevulinate enabled fluorescence cystoscopy. J Urol. 2012;188(1):58-62.
10. Picart T, Pallud J, Berthiller J, et al. Use of 5-ALA fluorescence-guided surgery versus white-light conventional microsurgery for the resection of newly diagnosed glioblastomas (RESECT study): a French multicenter randomized phase III study. J Neurosurg. 2024;140(4):987-1000.
11. Stummer W, Pichlmeier U, Meinel T, et al. Fluorescence-guided surgery with 5-aminolevulinic acid for resection of malignant glioma: a randomised controlled multicentre phase III trial. Lancet Oncol. 2006;7(5):392-401.
12. Lakomkin N, Van Gompel JJ, Post KD, Cho SS, Lee JYK, Hadjipanayis CG. Fluorescence guided surgery for pituitary adenomas. J Neurooncol. 2021;151(3):403-13.
13. Cho SS, Zeh R, Pierce JT, et al. Folate receptor near-infrared optical imaging provides sensitive and specific intraoperative visualization of non-functional pituitary adenomas. Oper Neurosurg (Hagerstown). 2019;16(1):59-70.
14. Johnston HE, Yadav K, Kirkpatrick JM, et al. Solvent precipitation SP3 (SP4) enhances recovery for proteomics sample preparation without magnetic beads. Anal Chem. 2022;94(29):10320-10328.
15. R Core Team. R: A language and environment for statistical computing. R Foundation for Statistical Computing, Vienna, Austria. 2017.
16. Zhang X, Smits AH, van Tilburg GB, Ovaa H, Huber W, Vermeulen M. Proteome-wide identification of ubiquitin interactions using UbIA-MS. Nat Protoc. 2018;13(3):530-550.
17. Ritchie ME, Phipson B, Wu D, et al. limma powers differential expression analyses for RNA-sequencing and microarray studies. Nucleic Acids Res. 2015;43(7):e47.
18. Wu T, Hu E, Xu S, et al. clusterProfiler 4.0: A universal enrichment tool for interpreting omics data. Innovation (Camb). 2021;2(3):100141.
19. Gene Ontology Consortium, Aleksander SA, Balhoff J, et al. The Gene Ontology knowledgebase in 2023. Genetics. 2023;224(1).
20. Yu G, Li F, Qin Y, Bo X, Wu Y, Wang S. GOSemSim: an R package for measuring semantic similarity among GO terms and gene products. Bioinformatics. 2010;26(7):976-978.
21. Chicco D, Agapito G. Nine quick tips for pathway enrichment analysis. PLoS Comput Biol. 2022;18(8):e1010348.
22. Reimand J, Isserlin R, Voisin V, et al. Pathway enrichment analysis and visualization of omics data using g:Profiler, GSEA, Cytoscape and EnrichmentMap. Nat Protoc. 2019;14(2):482-517.
23. Banerjee A, Biswas D, Barpanda A, et al. The first pituitary proteome landscape from matched anterior and posterior lobes for a better understanding of the pituitary gland. Mol Cell Proteomics. 2023;22(1):100478.
24. Zhang F, Zhang Q, Zhu J, et al. Integrated proteogenomic characterization across major histological types of pituitary neuroendocrine tumors. Cell Res. 2022;32(12):1047-1067.
25. Evans CO, Young AN, Brown MR, et al. Novel patterns of gene expression in pituitary adenomas identified by complementary deoxyribonucleic acid microarrays and quantitative reverse transcription-polymerase chain reaction. J Clin Endocrinol Metab. 2001;86(7):3097-3107.
26. Evans CO, Reddy P, Brat DJ, et al. Differential expression of folate receptor in pituitary adenomas. Cancer Res. 2003;63(14):4218-4224.
27. Vergeer RA, Postma MR, Schmidt I, et al. Detection by fluorescence of pituitary neuroendocrine tumour (PitNET) tissue during endoscopic transsphenoidal surgery using bevacizumab-800CW (DEPARTURE trial): study protocol for a non-randomised, non-blinded, single centre, feasibility and dose-finding trial. BMJ Open. 2021;11(10):e049109.
28. Cho SS, Jeon J, Buch L, et al. Intraoperative near-infrared imaging with receptor-specific versus passive delivery of fluorescent agents in pituitary adenomas. J Neurosurg. 2018;131(6):1974-1984.
29. Barry S, Korbonits M. Update on the genetics of pituitary tumors. Endocrinol Metab Clin North Am. 2020;49(3):433-452.
30. Blair JA, Wang C, Hernandez D, et al. Individual case analysis of postmortem interval time on brain tissue preservation. PLoS One. 2016;11(3):e0151615.

Dr Nicholas G. Candy
Department of Surgery
Otolaryngology, Head and Neck Surgery
The University of Adelaide
Basil Hetzel Institute for Translational Research
Woodville South
Adelaide
Australia

Tel: +61 432 605 173
E-mail:
Nicholas.candy@adelaide.edu.au

Nicholas G. Candy[1], Mahnaz Ramezanpour[1], George Bouras[1], Nusha Chegeni[2], Timothy Chataway[2], Rebecca J. Ormsby[3], Alistair K. Jukes[1], Sarah Vreugde[1], Peter-John Wormald[1], Alkis J. Psaltis[1]

[1] Department of Surgery - Otolaryngology, Head and Neck Surgery, The University of Adelaide, Basil Hetzel Institute for Translational Research, Woodville South, Adelaide, Australia

[2] Flinders Proteomic Facility, Department of Human Physiology, Flinders University, Bedford Park, Australia

[3] Flinders Health and Medical Research Institute, College of Medicine and Public Health, Flinders University, Adelaide, SA, Australia

Rhinology 62: 6, 750 - 758, 2024
https://doi.org/10.4193/Rhin24.216

Received for publication:
May 18, 2024
Accepted: August 5, 2024

Assocociate Editor:
Michael Soyka